Cold atoms in a two-dimensional triangular optical lattice as an artificial frustrated system

Yao-Hua Chen, Wei Wu, Hong-Shuai Tao, and Wu-Ming Liu

Beijing National Laboratory for Condensed Matter Physics, Institute of Physics, Chinese Academy of Sciences, Beijing 100190, China

(Received 3 May 2010; published 26 October 2010)

We investigate the strongly correlated effect of cold atoms in a triangular optical lattice using the dynamical cluster approximation combined with the continuous-time quantum Monte Carlo method. When the interaction increases, the Fermi surface evolves from a circular ring into a flat plane, and the system transitions from a Fermi liquid into a Mott insulator. The transition between the Fermi liquid and a pseudogap shows a reentrant behavior due to the Kondo effect. We give an experimental protocol to observe these phenomena in future experiments by varying the lattice depth and the atomic interaction via the Feshbach resonance.

DOI: 10.1103/PhysRevA.82.043625 PACS number(s): 67.85.−d, 03.75.Hh, 03.75.Ss, 71.10.Fd

I. INTRODUCTION

Quantum phase transition in a strongly correlated system is an important research area in condensed matter physics, and it presents some of the most challenging problems. In a real material, it is difficult to vary the experimental parameter to observe the strongly correlated effect, which is complicated by impurities and multiple bands. However, optical lattices present a highly controllable and clean system for studying a strongly correlated system in which the relevant parameter can be adjusted independently [1–6]. Optical lattices with different geometrical properties, such as such as triangular [7], honeycomb [8], and Kagomé [9–12] optical lattices, can be set up by adjusting the propagation directions of laser beams. The interaction between the trapped atoms is tunable through the Feshbach resonance, such as ^{6}Li and ^{40}K. In recent years, a series of experiments has been carried out to investigate the quantum phase transition of cold atoms in optical lattices [13–19].

There are many analytical and numerical methods used to investigate the strongly correlated system, especially the frustrated system [20–29]. The dynamical mean-field theory (DMFT) [30] has proven to be a useful tool. The self-energy is given as a local quantity in the DMFT, which has proved to be exact in the infinite-dimensional limit [31]. This method is a good approximation even for a three-dimensional situation [32]. However, in the frustrated systems, the nonlocal correlations cannot be simply ignored or the DMFT would not work efficiently. So, many methods have been improved to incorporate nonlocal correlations in the framework of DMFT, such as the dynamical cluster approximation (DCA) [33,34]. Differently from the DMFT, the lattice problem is mapped into a self-consistently embedded finite-sized cluster in the DCA. The irreducible quantities of the embedded cluster are used as an approximation for the corresponding lattice quantities. The DCA has been used to investigate the geometrical frustrated system [35,36].

In the present article, we investigate the Mott transition in an artificial frustrated system—cold atoms in a triangular optical lattice. We improve the numerical method, the DCA combined with the continuous-time quantum Monte Carlo method (CTQMC) [37], to investigate this geometrical frustrated system. The CTQMC, used as the impurity solver, is an exact numerical method that was proposed recently. By calculating the density of states and the spectral function, we find the system undergoes a second-order phase transition from Fermi liquid to Mott insulator. The phase diagram shows a reentrant behavior of the transition between the Fermi liquid and the pseudogap due to the Kondo effect at low temperature. These phenomena can be observed in the triangular optical lattice by varying the lattice depth and the interaction strength via the Feshbach resonance. The advantages of this artificial frustrated system are high controllabity and cleanliness, and the numerical method acts as a powerful tool for investigating the strongly correlated effect in condensed-matter physics, such as the spin liquid, the high-temperature superconductor, and the colossal magnetoresistance.

II. ARTIFICIAL FRUSTRATED SYSTEM

In contrast with real materials, the cold atoms trapped in an optical lattice provide an artificial system to investigate the strongly correlated effect. The experiment can be performed with ^{40}K atoms prepared by mixing two magnetic sublevels of the $F = 9/2$ hyperfine manifold, such as the $|-9/2\rangle$ and the $|-5/2\rangle$ states [16]. As an artificial frustrated system, the triangular optical lattice can be set up by three laser beams, such as the Yb fiber laser at wavelength $\lambda = 1064$ nm, with a $2\pi/3$ angle between each other, as illustrated in Fig. 1(a). The potential of optical lattice is given by

$$V(x,y) = V_0\left[3 + 4\cos\left(\frac{k_x x}{2}\right)\cos\left(\frac{\sqrt{3}k_y y}{2}\right) + 2\cos(\sqrt{3}k_y y)\right], \quad (1)$$

where V_0 is the barrier height of the standing wave formed by laser beams in the x-y plane, and k_x and k_y are the two components of the wave vector $k = 2\pi/\lambda$ along x and y directions. In experiments, V_0 is always given in units of recoil energy $E_r = \hbar^2k^2/2m$. The landscape of the potential of a triangular optical lattice in the x-y plane is shown in Fig. 1(b), where the dark blue parts in the figure indicate the minimum lattice potential. Figure 1(c) shows the contour lines of the triangular optical lattice. By connecting the center of the circular optical lattice, which indicates the minimum lattice potential, we may get the geometry of this triangular optical lattice, as shown by the red dashed lines.

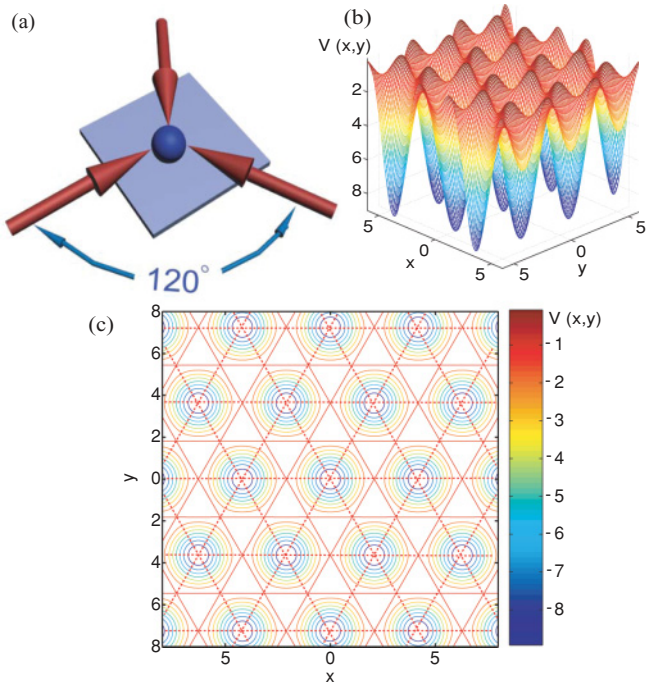

FIG. 1. (Color online) (a) A sketch of the experimental setup to form a triangular optical lattice. Each arrow depicts a laser beam; the sphere in the center of the figure depicts a fermionic quantum gas, such as ^{40}K. (b) Landscape of the potential $V(x,y)$. (c) The contour lines of a triangular optical lattice. The dark blue circles indicate the minimum lattice potential. The dashed red lines show the geometry of this triangular optical lattice by connecting the minimum lattice potential.

The Hamilitonian of the interacting fermionic atoms trapped in this artificial frustrated system is written as

$$H = -t \sum_{\langle ij\rangle\sigma} c^{\dagger}_{i\sigma} c_{j\sigma} + U \sum_{i} n_{i\uparrow} n_{i\downarrow}, \tag{2}$$

where $c^{\dagger}_{i\sigma}$ and $c_{i\sigma}$ denote the creation and the annihilation operator of the fermionic atom on lattice site i, respectively. $n_{i\sigma} = c^{\dagger}_{i\sigma} c_{i\sigma}$ represents the density operator of the fermionic atom, and $t = (4/\sqrt{\pi}) E_r (V_0/E_r)^{3/4} \exp[-2(V_0/E_r)^{1/2}]$ is the kinetic energy, which can be adjusted by the lattice depth V_0. $U = \sqrt{8/\pi} k a_s E_r (V_0/E_r)^{3/4}$ is the on-site interaction determined by the s-wave scattering length a_s, which can be adjusted by Feshbach resonance [6,38,39].

III. NUMERICAL METHOD: DCA + CTQMC

We improve the dynamical cluster approximation (DCA) to combine with the continuous-time quantum Monte Carlo method (CTQMC) to investigate the strongly correlated effect of cold atoms in the frustrated system shown in Fig. 2(a), which can be realized by the Hubbard model (2).

In the DCA, the reciprocal space of the lattice containing N points is divided into finite cells [34]. The coarse-graining Green's function $\overline{G}$ is achieved by averaging Green's function G within each cell. The lattice problem is mapped into a self-consistently embedded finite-sized cluster. The coarse-graining procedure of the DCA is illustrated as follows:

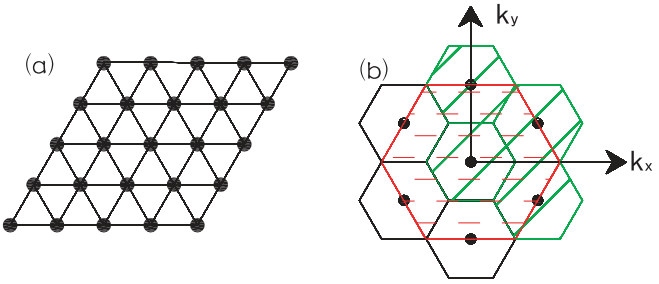

FIG. 2. (Color online) (a) Sketch of the triangular lattice. (b) A coarse-graining procedure in the first Brillouin zone when $N_c = 4$. The red dashed horizontal lines show the first Brillouin zone in reciprocal space. The green solid diagonal lines shows the region divided into four cells for the DCA calculation.

the Brillouin zone is divided into N_c cells, each cell represented by a cluster momentum $\vec{\mathbf{K}}$. In Fig. 2(b), we provide an example of this coarse-graining procedure in an $N_c = 4$ situation. In our treatment, the coarse-grained Green's function,

$$\begin{aligned}\overline{G}(\vec{\mathbf{K}}, i\omega_n) &= \frac{Nc}{N} \sum_{\tilde{\mathbf{k}}} G(\vec{\mathbf{K}} + \tilde{\mathbf{k}}, i\omega_n) \\ &= \frac{Nc}{N} \sum_{\tilde{\mathbf{k}}} \frac{1}{i\omega_n - \varepsilon_{\vec{\mathbf{K}}+\tilde{\mathbf{k}}} - \overline{\Sigma_\sigma}(\vec{\mathbf{K}}, i\omega_n)},\end{aligned} \tag{3}$$

where summation over $\tilde{\mathbf{k}}$ is taken within the coarse-graining cell, the ω_n is the Matsubara frequency.

Similar to the DMFT, after mapping the Hubbard model to an Anderson impurity problem we introduce an impurity solver to solve the cluster problem, such as the quantum Monte Carlo (QMC), the fluctuation exchange approximate (FLEX), and the noncrossing approximation (NCA). In our calculation, we employ the CTQMC [37] which does not need to introduce any anxiliary-field variables as our impurity solver. Compared to the traditional QMC method, the CTQMC is much more exact because it does not use the Trotter decomposition. We use 10^7 sweeps in our CTQMC step.

The self-consistent loop can be taken as follows:

(1) The DCA iteration loop can be started by setting the initial self-energy $\Sigma_c(\vec{\mathbf{K}}, i\omega_n)$, which can be guessed or gotten from a perturbation theory.

(2) We could get the following: $\overline{G}(\vec{\mathbf{K}}, i\omega_n) = \frac{Nc}{N} \sum_{\tilde{\mathbf{k}}} 1/[i\omega_n - \varepsilon_{\vec{\mathbf{K}}+\tilde{\mathbf{k}}} - \overline{\Sigma_\sigma}(\vec{\mathbf{K}}, i\omega_n)]$.

(3) The host Green's function $\overline{\mathcal{G}}(\vec{\mathbf{K}}, i\omega_n)$ is computed by $\overline{\mathcal{G}}(\vec{\mathbf{K}}, i\omega_n)^{-1} = \overline{G}(\vec{\mathbf{K}}, i\omega_n)^{-1} + \Sigma_c(\vec{\mathbf{K}}, i\omega_n)$.

(4) The $\overline{\mathcal{G}}(\vec{\mathbf{K}}, i\omega_n)$ is transformed from a momentum-frequency variable to a space-time variable $\overline{\mathcal{G}}(\vec{\mathbf{X}}_i - \vec{\mathbf{X}}_j, \tau_i - \tau_j)$ used as the input to the CTQMC simulation.

(5) The CTQMC step is the most time-consuming part of the iteration loop. In our CTQMC step, we use 10^7 CTQMC sweeps. After the simulation, we get $\overline{G}(\vec{\mathbf{X}}_i - \vec{\mathbf{X}}_j, \tau_i - \tau_j)$.

(6) $\overline{G}(\vec{\mathbf{X}}_i - \vec{\mathbf{X}}_j, \tau_i - \tau_j)$ is transformed from a space-time variable to a momentum-frequency variable $\overline{G}(\vec{\mathbf{K}}, i\omega_n)$ by Fourier transform.

(7) We get the new self-energy by $\Sigma_c(\vec{\mathbf{K}}, i\omega_n) = \overline{\mathcal{G}}(\vec{\mathbf{K}}, i\omega_n)^{-1} - \overline{G}(\vec{\mathbf{K}}, i\omega_n)^{-1}$.

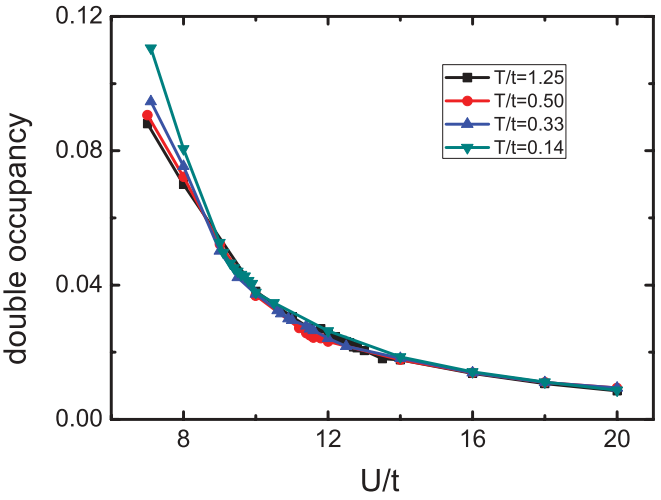

FIG. 3. (Color online) The double occupancy $D_{\rm occ}$ as a function of the interaction U for different temperature. t is the kinetic energy in Eq. (2).

(8) Repeat from steps (2) to (7) until $\Sigma_c(\vec{\mathbf{K}}, i\omega_n)$ converges to the desired accuracy.

(9) Once convergence is reached, we can calculate the state density $\rho(\omega)$ by the maximum entropy method [40]. And we can get other lattice quantities by some other additional analysis code.

By combining the DCA, which introduces the nonlocal correlations, and the exact numerical method, CTQMC, we can investigate the frustrated system efficiently. This numerical method can be easily reconstructed to study another strongly correlated system in future research.

IV. PHASE DIAGRAM

We investigate the double occupancy $D_{\rm occ} = \partial F/\partial U = \frac{1}{4}\sum_i \langle n_{i\uparrow} n_{i\downarrow}\rangle$ as a function of interaction U for various temperatures, where F is the free energy. When the interaction is lower than $U/t = 8.6$, the $D_{\rm occ}$ increases as the temperature decreases due to the enhancing of the itinerancy of atoms, as shown in Fig. 3. When the interaction is stronger than $U/t = 8.6$, the effect of the temperature on $D_{\rm occ}$ is weakened. The $D_{\rm occ}$ decreases as the interaction increases due to the suppressing of the itinerancy of the atoms. When the interaction is stronger than the critical interaction of the Mott transition, $D_{\rm occ}$ for different temperatures is coincident, which shows the temperature does not affect the double occupancy distinctly. The continuity of the evolution of the double occupancy by interaction shows that it is a second-order transition.

We employ the maximum entropy method [40] to calculate the density of states (DOS) which describes the number of states at frequency ω. Figure 4(a) shows the DOS for different interactions at $T/t = 0.5$. There is a Fermi-liquid-like peak when $U/t = 4.0$. A pseudogap formed by the splitting of Fermi-liquid-like peak appears when the interaction increases, such as $U/t = 8.0$ and $U/t = 9.0$. When the interaction is stronger than the critical interaction $U_c/t = 11.6$, such as $U/t = 12.0$ and $U/t = 20.0$, the system becomes an insulator indicated by an opened gap. The DOS for different interactions

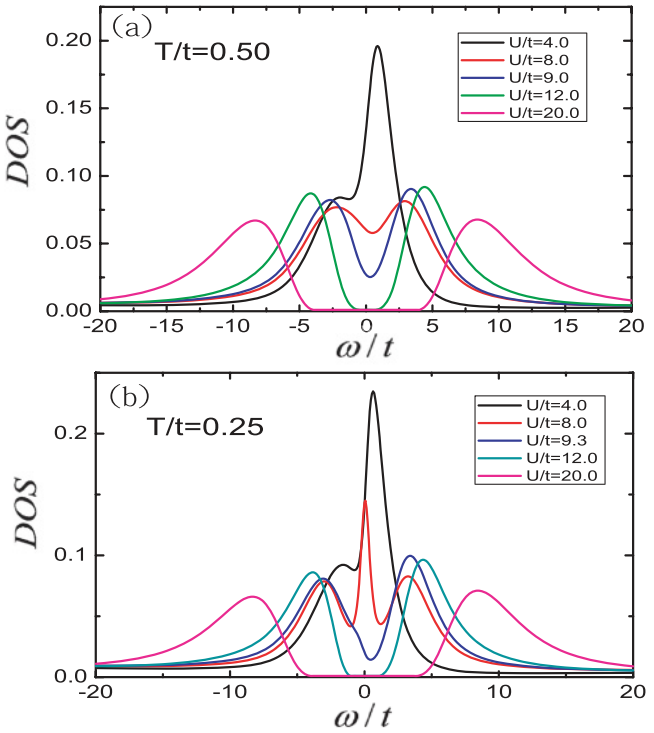

FIG. 4. (Color online) The density of states (DOS) as a function of frequency ω for different interactions. t is the kinetic energy in Eq. (2). (a) At $T/t = 0.50$, a pseudogap formed by the splitting of Fermi-liquid-like peak appears when the interaction increases. A gap is opened when the interaction is stronger than the critical interaction $U_c/t = 11.6$. (b) At $T/t = 0.25$, a Kondo resonance peak is found before the pseudogap appears.

at $T/t = 0.25$ is shown in Fig. 4(b). When $U/t = 4.0$, there is also a Fermi-liquid-like peak. When the interaction increases, such as $U/t = 8.0$, a Kondo resonance peak appears which is shown by a sharp quasiparticle peak with two shoulders. When $U/t = 9.3$, the Kondo resonance peak is suppressed and a pseudogap appears, which is the intermediary state between the Fermi liquid and the Mott insulator. A gap is opened when the interaction is stronger than the critical interaction $U_c/t = 10.6$. Instead of directly splitting into two parts shown in Fig. 4(a), a Kondo peak appears, which is formed by the effect between the local atom and the itinerant atom at low temperature, as shown in Fig. 4(b).

We could also get the K-dependent spectral function $A_k(\omega) = -\mathrm{Im}\,\mathrm{G_k}(\omega + \mathrm{i}0)/\pi$, which describes the distribution probability of the quasiparticle with momentum k and energy ω. Figure 5 shows $A_k(\omega)$ for different temperature, where $U/t = 7.0$. At $T/t = 1.67$, there exists a quasiparticle peak which shows a metallic behavior, as shown in Fig. 5(a). In Fig. 5(b), a pseudogap appears at $T/t = 1.11$, which is formed by the splitting of the quasiparticle peak. When $T/t = 0.50$, the pseudogap disappears and there is a quasiparticle peak again, as shown in Fig. 5(c). An obvious Kondo peak appears when $T/t = 0.2$, as shown in Fig. 5(d). It shows a reentrant behavior in the transition between the Fermi liquid and the pseudogap when the interaction is fixed and the temperature decreases. This behavior is based on the Kondo effect which

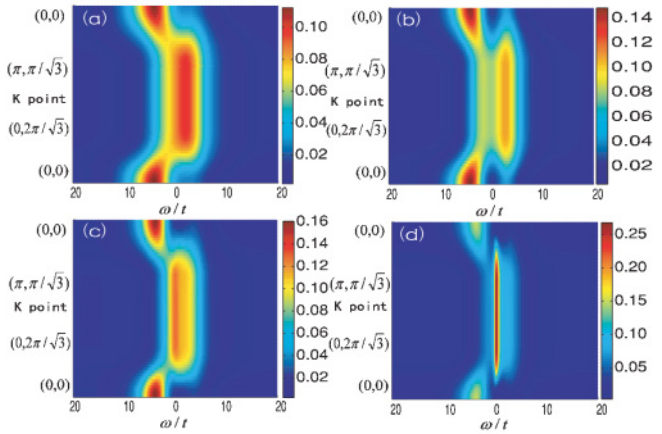

FIG. 5. (Color online) The K-dependent spectral function $A_k(\omega)$ for different temperatures when $U/t = 7.0$. t is the kinetic energy in Eq. (2). (a) At $T/t = 1.67$, the red region (near $\omega/t = 1.5$) shows a Fermi-liquid-like peak near Fermi energy. (b) At $T/t = 1.11$, a narrow pesudogap is shown by the green region (near $\omega/t = 0$). Two peaks found around the pesudogap are shown by yellow (near $\omega/t = -2$) and orange (near $\omega/t = 2.5$). (c) At $T/t = 0.5$, a Fermi-liquid-like peak appears again shown by red (near $\omega/t = 0$). (d) At $T/t = 0.2$, an obvious Kondo peak appears shown by red (near $\omega/t = 0$).

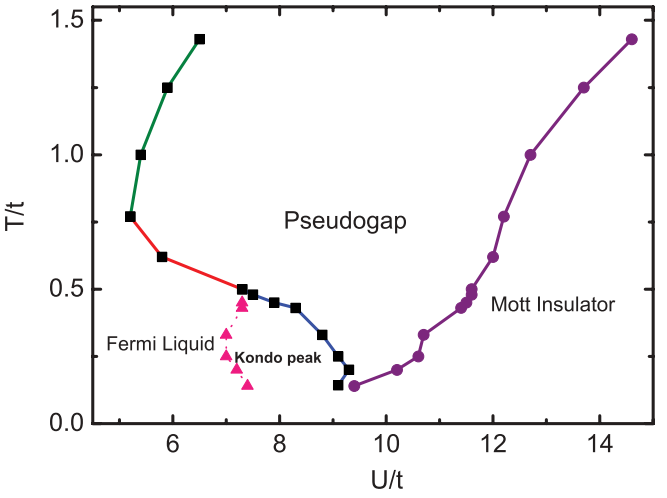

FIG. 7. (Color online) The phase diagram of Fermi atoms in a triangular optical lattice, where the square plots on the solid line (green, red, blue) indicate the transition line of the Fermi liquid and the pseudogap, the circular plots on the solid line (purple) indicate the Mott transition line, and the triangular plots on the dashed line (pink) mark the Kondo peak appearing region. t is the kinetic energy in Eq. (2).

suppresses the splitting of the quasiparticle peak at low temperature.

We study the Fermi surface as a function of momentum k by $A(k;\omega = 0) \approx -\frac{1}{\pi} \lim_{w_n \to 0} \mathrm{Im}G(k, i\omega_n)$. A linear extrapolation of the first two Matsubara frequencies is used to estimate the self-energy to zero frequency [41]. Figure 6 shows the Fermi surface for a different interaction at $T/t = 1.25$. A circular ring, which means the particles distribute on a certain energy, displays a metallic behavior, as shown in Fig. 6(a-1). As the interaction increases, the ring becomes bigger, as shown in Fig. 6(b-1). When the interaction is stronger than the critical interaction $U/t = 13.7$, the Fermi surface becomes a nearly flat plane, as shown in Fig. 6(c-1). From Figs. 6(a-2) to 6(c-2), we find that the amplitude of the spectral weight becomes smaller and the breadth becomes wider. The Fermi surface transitions from a determined surface into a flat plane

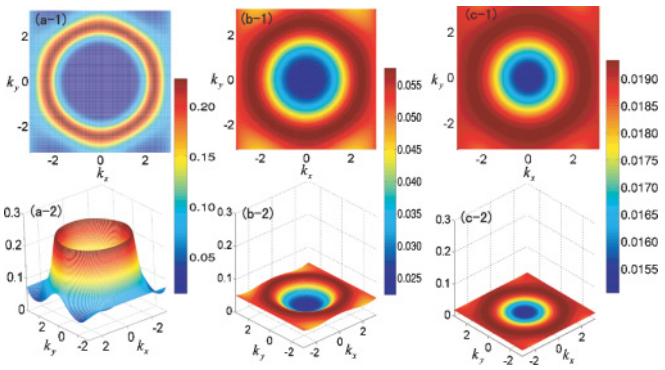

FIG. 6. (Color online) The Fermi surface as a function of momentum k for different interaction at $T/t = 1.25$: (a) $U/t = 5.0$, (b) $U/t = 10.0$, (c) $U/t = 16.0$. t is the kinetic energy in Eq. (2).

due to the localization of the particles when the interaction increases.

The phase diagram of cold atoms trapped in a triangular optical lattice is shown in Fig. 7, where a_s indicates the s-wave scattering length. The transition between the Fermi liquid and the pseudogap shows a reentrant behavior. For a fixed interaction weaker than $U/t = 7.2$, when the temperature decreases, the system transitions from a Fermi liquid to a pseudogap. When the temperature is lower than the critical temperature distributing on the red solid line, the system transitions from pesudogap to Fermi liquid. There is a Kondo peak region, which is indicated by the blue solid line and the pink dashed line. If the temperature is lower than $T/t = 2.0$, a Kondo peak emerges before the appearing of the pseudogap when the interaction increases. When the interaction is stronger than the critical interaction of the Mott transition distributing on the purple line, the system translates from a pseudogap to an insulator confirmed by an opened gap.

V. EXPERIMENTAL PROTOCOL

We designed an experiment to investigate the quantum phase transition in a triangular optical lattice. The experimental protocol can be taken as follows: The ^{40}K atoms can be produced as a pure fermion condensate by evaporative cooling [42]. Three laser beams at wavelength $\lambda = 1064$ nm are used to form the triangular optical lattice [43] to trap ^{40}K atoms. The lattice depth V_0 is used to adjust the kinetic energy t and the interaction U. The on-site interaction can be adjusted by Feshbach resonance [44–48]. The s-wave scattering length is used to determine the effective interaction. The temperature can be extracted from time-of-flight images by means of Fermi fits in experiment [19].

When the interaction increases, the system transitions from a Fermi liquid ($a_s < 48a_0$) to a Mott insulator ($a_s > 111a_0$) at temperature $T = 5.96$ nK, when $V_0 = 10E_r$. In order to detect the double occupancy $D_{\rm occ}$, we rapidly increase the depth of the optical lattice to prevent further tunneling. Next we shift the energy of the atoms on doubly occupied sites by approaching a Feshbach resonance. Then one spin component of the atoms on the double occupied sites is transferred to an unpopulated magnetic sublevel by using a radio-frequency pulse. The double occupancy can be deduced by the fraction of transformed atoms obtained by the absorption imagining [16,49]. At $T = 5.96$ nK, $D_{\rm occ}$ decreases from 0.110 09 ($a_s = 45a_0$) to 0.004 56 ($a_s = 130a_0$) with increasing atomic interaction.

By ramping down the optical lattice slowly enough, the atoms stay adiabatically in the lowest band while the quasimomentum is approximately conserved. Then, the optical lattice is converted from a deep one into a shallow one and the quasimomentum is preserved. After completely turning off the confining potential, the atoms ballistically expand for several milliseconds. Then by absorption imagining, one can get the Fermi surface [50,51]. At $T = 5.96$ nK, the circular ring shape of the Fermi surface when $a_s = 41a_0$ transforms into a flat plane when $a_s = 162a_0$.

VI. SUMMARY

In summary, we investigate the Mott transition of the cold atoms in a two-dimensional triangular optical lattice set up by three laser beams. The system evolves from a Fermi liquid into a Mott insulator for increasing interaction, and a reentrant behavior of the transition between Fermi liquid and the pesudogap is found due to the Kondo effect. Our study presents a helpful step for understanding the strongly correlated effect in the frustrated system, such as the spin liquid. Beyond the DMFT, the DCA is improved to incorporate the nonlocal correlation which cannot be simply ignored in the frustrated system. This numerical method is universally used to investigate strongly correlated systems, such as the high-temperature superconductor and the colossal magnetoresistance.

ACKNOWLEDGMENTS

This work was supported by NSFC under Grants No. 10874235, No. 10934010, and No. 60978019, and the NKBRSFC under Grants No. 2011CB921500, No. 2009CB930701, and No. 2010CB922904.

[1] D. Jaksch, C. Bruder, J. I. Cirac, C. W. Gardiner, and P. Zoller, Phys. Rev. Lett. **81**, 3108 (1998).
[2] K. I. Petsas, A. B. Coates, and G. Grynberg, Phys. Rev. A **50**, 5173 (1994).
[3] W. Hofstetter, J. I. Cirac, P. Zoller, E. Demler, and M. D. Lukin, Phys. Rev. Lett. **89**, 220407 (2002).
[4] Y. Inada, M. Horikoshi, S. Nakajima, M. Kuwata-Gonokami, M. Ueda, and T. Mukaiyama, Phys. Rev. Lett. **101**, 180406 (2008).
[5] M. Kottke, T. Schulte, L. Cacciapuoti, D. Hellweg, S. Drenkelforth, W. Ertmer, and J. J. Arlt, Phys. Rev. A **72**, 053631 (2005).
[6] I. Bloch, J. Dalibard, and W. Zwerger, Rev. Mod. Phys. **80**, 885 (2008).
[7] D. Joksch and P. Zoller, Ann. Phys. (NY) **315**, 52 (2005).
[8] L. M. Duan, E. Demler, and M. D. Lukin, Phys. Rev. Lett. **91**, 090402 (2003).
[9] L. Santos, M. A. Baranov, J. I. Cirac, H. U. Everts, H. Fehrmann, and M. Lewenstein, Phys. Rev. Lett. **93**, 030601 (2004).
[10] B. Damski, H. Fehrmann, H. U. Everts, M. Baranov, L. Santos, and M. Lewenstein, Phys. Rev. A **72**, 053612 (2005).
[11] B. Damski, H. U. Everts, A. Honecker, H. Fehrmann, L. Santos, and M. Lewenstein, Phys. Rev. Lett. **95**, 060403 (2005).
[12] J. Ruostekoski, Phys. Rev. Lett. **103**, 080406 (2009).
[13] M. Greiner, O. Mandel, T. Esslinger, T. W. Hänsch, and I. Bloch, Nature (London) **415**, 39 (2002).
[14] D. Hellweg, L. Cacciapuoti, M. Kottke, T. Schulte, K. Sengstock, W. Ertmer, and J. J. Arlt, Phys. Rev. Lett. **91**, 010406 (2003).
[15] Y. Shin, C. H. Schunck, A. Schirotzek, and W. Ketterle, Nature (London) **451**, 689 (2008).
[16] R. Jördans, N. Strohmaier, K. Günter, H. Moritz, and T. Esslinger, Nature (London) **455**, 204 (2008).
[17] N. Gemelke, X. Zhang, C. L. Hung, and C. Chin, Nature (London) **460**, 995 (2009).
[18] R. Jördens *et al.*, Phys. Rev. Lett. **104**, 180401 (2010).
[19] U. Schneider, L. Hackermller, S. Will, Th. Best, I. Bloch, T. A. Costi, R. W. Helmes, D. Rasch, and A. Rosch, Science **322**, 1520 (2009).
[20] T. Ohashi, T. Momoi, H. Tsunetsugu, and N. Kawakami, Phys. Rev. Lett. **100**, 076402 (2008).
[21] T. Yoshioka, A. Koga, and N. Kawakami, Phys. Rev. Lett. **103**, 036401 (2009).
[22] D. Galanakis, T. D. Stanescu, and P. Phillips, Phys. Rev. B **79**, 115116 (2009).
[23] K. Aryanpour, W. E. Pickett, and R. T. Scalettar, Phys. Rev. B **74**, 085117 (2006).
[24] S. G. Bhongale and H. Pu, Phys. Rev. A **78**, 061606 (2008).
[25] P. B. He, Q. Sun, P. Li, S. Q. Shen, and W. M. Liu, Phys. Rev. A **76**, 043618 (2007).
[26] V. V. Konotop and M. Salerno, Phys. Rev. A **65**, 021602 (2002).
[27] Y. Kato, Q. Zhou, N. Kawashima, and N. Trivedi, Nat. Phys. **4**, 617 (2008).
[28] Z. D. Li, Q. Y. Li, P. B. He, J. Q. Liang, W. M. Liu, and G. S. Fu, Phys. Rev. A **81**, 015602 (2010).
[29] T. Ohashi, N. Kawakami, and H. Tsunetsugu, Phys. Rev. Lett. **97**, 066401 (2006).
[30] A. Georges, G. Kotliar, W. Krauth, and M. J. Rozenberg, Rev. Mod. Phys. **68**, 13 (1996).
[31] W. Metzner and D. Vollhardt, Phys. Rev. Lett. **62**, 324 (1989).
[32] R. W. Helmes, T. A. Costi, and A. Rosch, Phys. Rev. Lett. **100**, 056403 (2008).
[33] T. Maier, M. Jarrell, T. Pruschke, and M. H. Hettler, Rev. Mod. Phys. **77**, 1027 (2005).
[34] M. Jarrell and H. R. Krishnamurthy, Phys. Rev. B **63**, 125102 (2001).
[35] Y. Imai and N. Kawakami, Phys. Rev. B **65**, 233103 (2002).
[36] H. Lee, G. Li, and H. Monien, Phys. Rev. B **78**, 205117 (2008).

[37] A. N. Rubtsov, V. V. Savkin, and A. I. Lichtenstein, Phys. Rev. B **72**, 035122 (2005).
[38] L. M. Duan, Phys. Rev. Lett. **95**, 243202 (2005).
[39] C. Chin, R. Grimm, P. Julienne, and E. Tiesinga, Rev. Mod. Phys. **82**, 1225 (2010).
[40] M. Jarrell and J. E. Gubernatis, Phys. Rep. **269**, 133 (1996).
[41] O. Parcollet, G. Biroli, and G. Kotliar, Phys. Rev. Lett. **92**, 226402 (2004).
[42] K. M. O'Hara, S. L. Hemmer, M. E. Gehm, S. R. Granade, and J. E. Thomas, Science **298**, 2179 (2002).
[43] S. Tung, V. Schweikhard, and E. A. Cornell, Phys. Rev. Lett. **97**, 240402 (2006).
[44] T. Loftus, C. A. Regal, C. Ticknor, J. L. Bohn, and D. S. Jin, Phys. Rev. Lett. **88**, 173201 (2002).
[45] M. W. Zwierlein, A. Schirotzek, C. H. Schunck, and W. Ketterle, Science **311**, 492 (2006).
[46] C. A. Regal, C. Ticknor, J. L. Bohn, and D. S. Jin, Nature (London) **424**, 47 (2003).
[47] C. Klempt, T. Henninger, O. Topic, J. Will, W. Ertmer, E. Tiemann, and J. Arlt, Phys. Rev. A **76**, 020701 (2007).
[48] T. Stöferle, H. Moritz, K. Günter, M. Köhl, and T. Esslinger, Phys. Rev. Lett. **96**, 030401 (2006).
[49] N. Strohmaier, Y. Takasu, K. Günter, R. Jördens, M. Köhl, H. Moritz, and T. Esslinger, Phys. Rev. Lett. **99**, 220601 (2007).
[50] M. Köhl, H. Moritz, T. Stöferle, K. Günter, and T. Esslinger, Phys. Rev. Lett. **94**, 080403 (2005).
[51] J. K. Chin, D. E. Miller, Y. Liu, C. Stan, W. Setiawan, C. Sanner, K. Xu, and W. Ketterle, Nature (London) **443**, 961 (2006).